Journal of the Geological Society, London, Vol. **148,** 1991, pp. 643–653, 10 figs, 1 table. Printed in Northern Ireland

Modern and ancient continental hypsometries

T. J. ALGEO & B. H. WILKINSON
Department of Geological Sciences, University of Michigan, Ann Arbor, Michigan 48109-1063 USA

Abstract: Controls on coastal hypsometries of modern continents and oceanic islands may be used to estimate palaeo-continental area-elevation distributions. The most important controls on coastal hypsometry are landmass area and coastal gradient, increases in which result in steeper area-elevation distributions. Thus, any change in sea level will flood or expose a smaller fractional area of continents which are large or have steep coastal gradients than of those which are small or have gentle coastal gradients. Coastal gradients are dictated primarily by the tectonic setting and age of continental margins. While active and transform margins generally have steep coasts, mean coastal gradients for passive margins decrease exponentially with increasing margin age. Consequently, continents comprised mostly of mature passive margins are generally more 'floodable'.

These observations are applicable to a variety of palaeo-eustatic problems. Hypsometries corrected for changes in landmass area reduce variance in flooding records between different Palaeozoic continents by more than 50%. Assuming minimum-variance superimposition of flooding curves for different Palaeozoic continents permits identification of possible hypsometric anomalies. Calculated Palaeozoic sea level maxima are between +200 m and +400 m with respect to present sea level, substantially lower than previous estimates to +600 m.

Modelling evolution of coastal hypsometries due to changes in length and age of passive margins suggests that hypsometry varies cyclically in response to continental rifting and collision. Coastal hypsometries are steepest during rifting events and decrease by a factor of two to three as passive margins age. Coastal hypsometries in a 'sutured' world are steeper than those of a 'rifted' world due to increased continent size and decreased passive margin length. Thus, sea level highstands associated with times of continent dispersal may result in part from the enhanced 'floodability' of rifted continents.

Hypsometry is the distribution of area with respect to elevation for a topographic surface. Combined with continental flooding data, hypsometry can be used to determine sea level elevation (Fig. 1). The technique utilizes palaeogeographic maps which show an interpolated shoreline based on the distribution of marine and continental facies of a given age, and from which fractional land area flooded is measured directly. A landmass-specific hypsometric curve is then used to convert fractional area flooded to sea level elevation. In this manner, a continuous sea level curve can be constructed from a series of palaeogeographic maps for successive geologic epochs (Fig. 1).

Hypsometry and continental flooding data thus permit direct quantification of palaeo-sea levels. Integration of flooding data over large, relatively stable cratonic areas avoids many of the difficulties inherent in seismic stratigraphic studies due to conflation of absolute sea level changes with passive margin subsidence (Pitman 1978). While hypsometry does not yield as detailed a sea level record as do seismic or sequence stratigraphic analysis, it is probably the best method for estimating the amplitudes of long-period (i.e. >10 Ma) sea level changes. Furthermore, the technique is applicable to the entire Phanerozoic, unlike methods based on passive margin seismic stratigraphy (Vail *et al.* 1977; Haq *et al.* 1987) and mid-ocean ridge volume analysis (Pitman 1978). Derivation of a reasonably accurate record of long-period Phanerozoic eustasy is critical to our understanding of such diverse phenomena as secular changes in oceanic and atmospheric chemistry (Berner *et al.* 1983), species diversity and extinction events (Wyatt 1987; Schopf 1974), and sedimentation patterns (Shanmugam & Moiola 1982).

The most fundamental problem inherent in hypsometric investigations of palaeo-eustasy is the absence of any record of ancient area-elevation distributions. In contrast, modern hypsometries of individual continents and of the globe as a whole are well-established (Kossinna 1933; Harrison *et al.* 1983; Cogley 1985), and have been employed without modification in all hypsometric studies of palaeo-eustasy known to us (Forney 1975; Bond 1978*a*, *b*; Harrison *et al.* 1981, 1983; Hallam 1984). In these studies, any change in freeboard for a given landmass is assumed to be a direct reflection of comparable eustatic change, and a temporally-invariant hypsometric curve serves only to convert fractional area flooded to sea level elevation.

In reality, continental hypsometries have probably evolved through time due to such geotectonic and geomorphological factors as rifting and suturing of landmasses, changes in type and age of continental margins, and uplift and peneplanation of cratonic interiors. While unlikely, it is at least conceivable that Phanerozoic sea level has remained approximately constant and that changes in continental flooding have resulted primarily from changes in hypsometry. More probably, continental flooding records the interaction of these two phenomena, and attempts to extract sea level from flooding data will be unsatisfactory unless hypsometric changes are taken into account.

What is required is knowledge of changes in continental hypsometries through time, but no direct record of such variation exists and it is necessary to find one or more proxy indicators which yield acceptable estimates of palaeo-

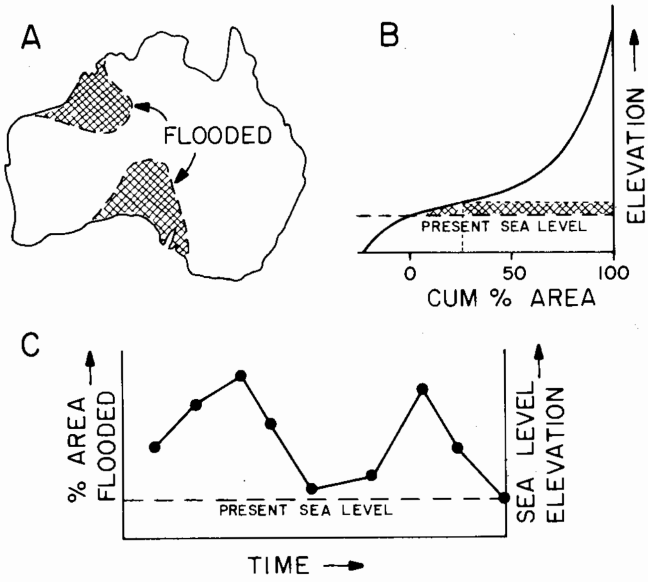

Fig. 1. Example of sea level determination using hypsometry and area-flooded data. (**A**) Percent area flooded for a given epoch measured from an equal-area palaeogeographic map. (**B**) Percent area flooded converted to sea level elevation using a landmass-specific hypsometric curve. (**C**) Sea level curve constructed from a series of palaeogeographic maps.

hypsometry. We approach this problem by analyzing the coastal hypsometries of modern continents and oceanic islands. Our goals are: (1) to establish the geometric and geotectonic controls on modern area-elevation distributions, (2) to demonstrate their utility as proxy indicators of palaeo-hypsometry for Palaeozoic landmasses, and (3) to constrain the range of probable changes in hypsometry through a full geotectonic (i.e. Wilson) cycle.

Sea level and hypsometry

Hypsometric slope

Harrison *et al.* (1981) recognized that major changes in global hypsometry may occur during the course of geotectonic cycles and attempted to quantify the effect on the global hypsometric curve of putting all landmasses into a single continent (e.g. Permo-Triassic Pangaea). They postulated that a supercontinent would have a higher rate of change of elevation with respect to fractional land area, and that larger sea level changes would be necessary to flood or expose a given percentage of total area. We formalize the idea of the rate of change of elevation with respect to fractional area as 'hypsometric slope', which has dimensions of metres per percent area. In theory, it is an instantaneous measurement as hypsometric slope changes continuously with changes in elevation. In practice, continental areas have been determined only at elevation intervals of 100 m (Harrison *et al.* 1983), and their derivative hypsometric slopes are thus calculable only for a range of elevations of 100 m or more. For all continents, hypsometric slope is relatively gentle at low elevations and steepens rapidly at higher elevations (Harrison *et al.* 1981). Significantly, at any given elevation, there are large differences in hypsometric slope for different continents, resulting in variable rates of flooding or exposure due to eustatic change (Fig. 2).

In eustatic studies, only low-elevation areas are of significance. Examination of modern continental hypsometric curves shows that each continent exhibits a relatively uniform hypsometric slope over an elevation range from −50 m to +250 m with respect to present-day sea level (Fig. 2; Harrison *et al.* 1983). As a consequence, sea level changes within this range produce linear changes in area flooded for each continent at a continent-specific rate. This observation is the basis for determining a 'coastal zone' hypsometric slope for each landmass. While Phanerozoic sea levels may occasionally have exceeded this elevation range (Hallam 1984), global sea level has oscillated within a fairly narrow

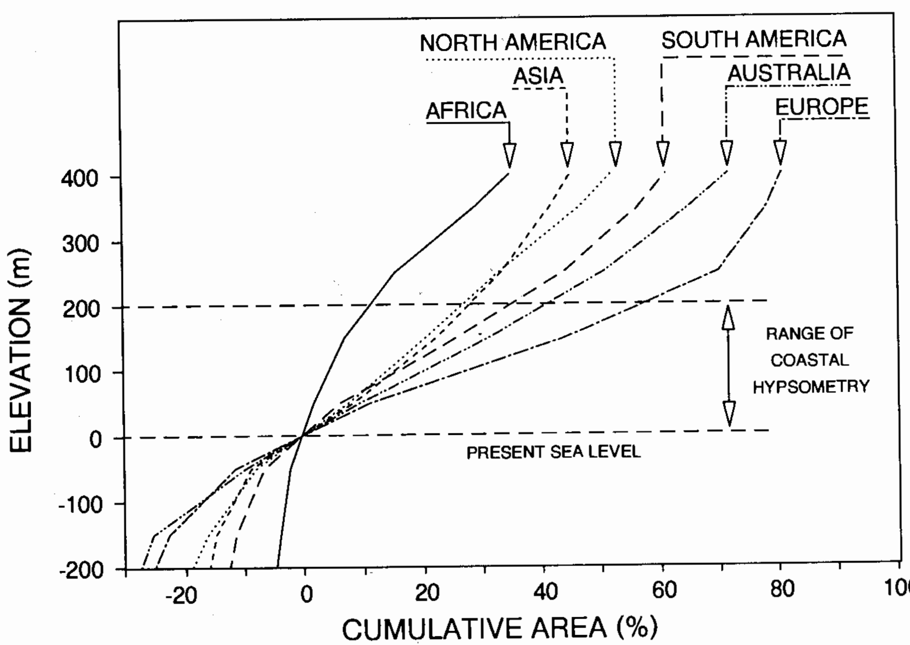

Fig. 2. Hypsometric curves of present-day continents from −200 m to +400 m with respect to sea level. Note that hypsometric slope, or the rate of change of elevation with respect to fractional area, is relatively constant for each continent from −50 m to +250 m but varies substantially between continents. 'Coastal hypsometries' were determined for the elevation range 0–200 m. Data from Harrison *et al.* (1983).

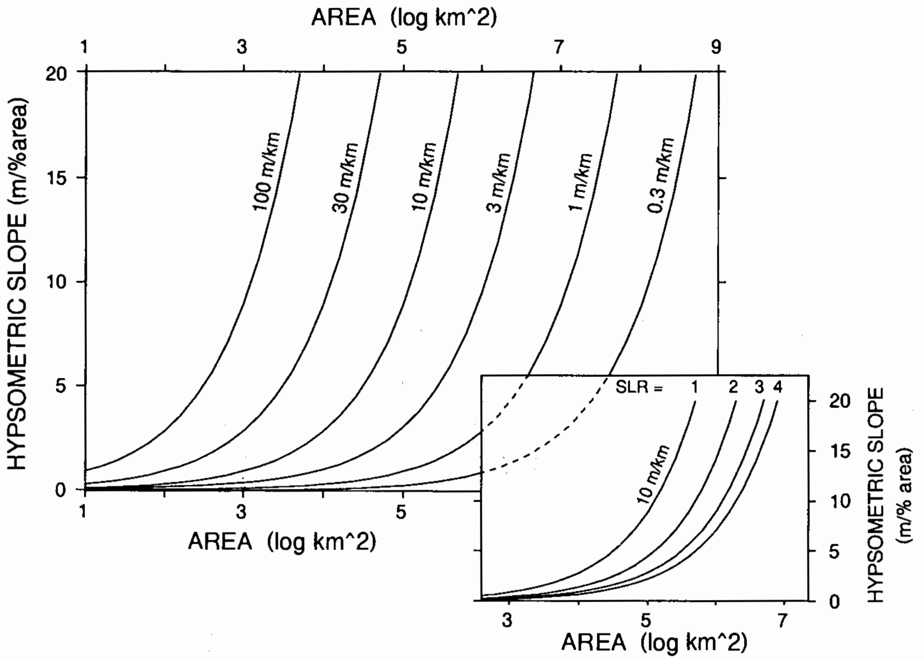

Fig. 4. Model hypsometric slopes resulting from various combinations of three geometric parameters. Main figure shows change in hypsometric slope due to increasing landmass area for six different values of coastal gradient (shoreline ratio is constant and equal to 1.0). Figure offset to lower right shows hypsometric slopes resulting from increasing landmass area for four different values of shoreline ratio (coastal gradient is constant and equal to 10 m km^{-1}). These parameter ranges bracket those of most present-day landmasses.

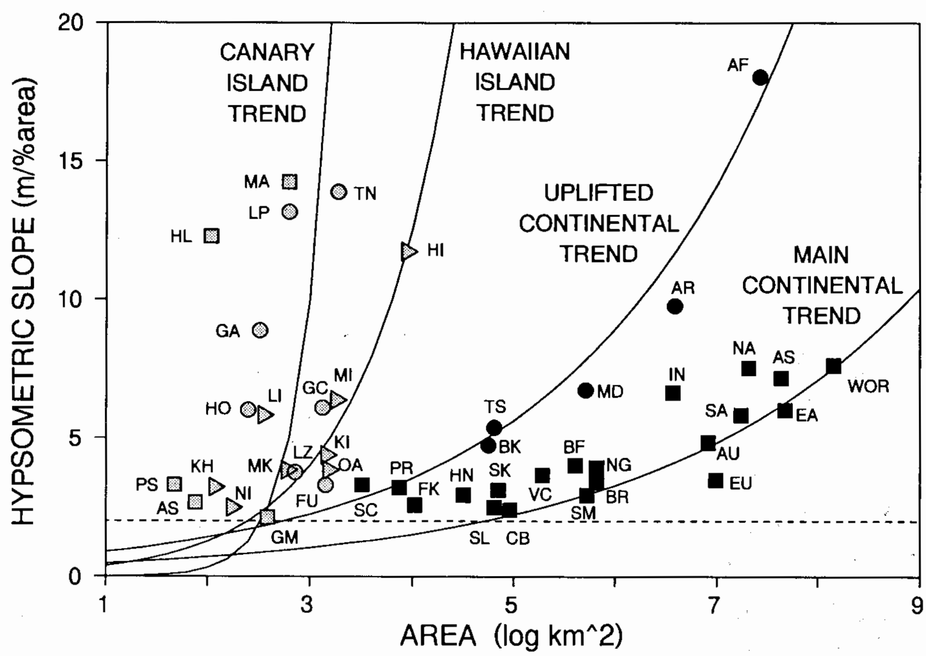

Fig. 5. Hypsometric slope versus area for modern landmasses. Oceanic islands are shown by shaded symbols (Canary Islands, circles; Hawaiian Islands, triangles; Other islands, squares). Uplifted continents are shown by solid circles and main trend continents by solid squares. Oceanic Islands: (Canary Is.) FU, Fuerteventura; GA, Gomera; GC, Gran Canaria; Ho, Hierro; LP, La Palma; LZ, Lanzarote; TN, Tenerife; (Hawaiian Is.) HI, Hawaii; KH, Kahoolawe; KI, Kauai; LI, Lanai; MI, Maui; MK, Molokai; NI, Niihau; OA, Oahu; (Others) AS, Ascension; GM, Guam; HL, St Helena; MA, Madeira; PS, Porto Santo. Continents: AF, Africa; AR, Arabia; AS, Asia; AU, Australia; BF, Baffin; BK, Banks; BR, Borneo; CB, Cuba; EA, Eurasia; EU, Europe; FK, Falklands; HN, Hainan; IN, India; MD, Madagascar; NA, North America; NG, New Guinea; PR, Puerto Rico; SA, South America; SC, Socotra; SK, Sakhalin; SL, Sri Lanka; SM, Sumatra; TS, Tasmania; VC, Victoria; WOR, World. Area-elevation distributions from Harrison *et al.* (1983) and *Times Atlas of the World* (1985).

Empirically-fit curves model hypsometric slope trends for four different landmass groups. Curve parameters: (1) Hawaiian Island Trend: CG (coastal gradient) = 1.65 m km^{-1}, $CG \propto AR^0$ (area); (2) Canary Island trend: $CG = 1.65$ log m km^{-1} at 400 km^2, $CG \propto AR^1$; (3) Main continental trend: $CG = -0.60$ log m km^{-1} at 1×10^8 km^2, $CG \propto AR^{-0.33}$; (4) Uplifted continental trend: $CG = 0.20$ log m km^{-1} at 1×10^7 km^2, $CG \propto AR^{-0.30}$. The dashed horizontal line represents the hypsometric slope 'floor;' no landmass with a maximum elevation less than 200 m was considered and, thus, no hypsometric slope less than 2.0 m/%area was possible.

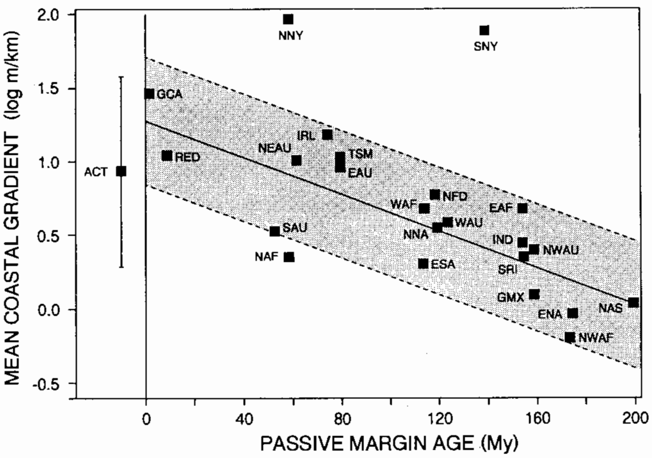

Fig. 7. Relationship of coastal gradient to passive margin age. Mean coastal gradient decreases exponentially with increasing margin age (note that the ordinate has a logarithmic scale). The equation of the regression line (solid) is $Y = -0.0062 \times X + 1.28$; its correlation coefficient is -0.80. Coastal gradient standard deviations are not age-dependent; therefore, the mean standard deviation (0.42 log m km^{-1}) is shown as an envelope (shaded) around the regression line. Mean coastal gradients for Northern and Southern Norway (NNY and SNY) were excluded from regression calculations. The mean and standard deviation envelope for active and transform margins are shown on left side of figure. ACT, Active/transform margins; EAF, Eastern Africa; EAU, Eastern Australia; ENA, Eastern North America; ESA, Eastern South America; GCA, Gulf of California; GMX, Gulf of Mexico; IND, India; IRL, Ireland; NAF, Northern Africa; NAS, Northern Asia (Arctic); NEAU, Northeastern Australia; NFD, Newfoundland; NNA, Northern North America (Arctic); NNY, Northern Norway (Atlantic); NWAF, Northwest Africa; NWAU, Northwestern Australia; RED, Red Sea; SAU, Southern Australia; SNY, Southern Norway (North Sea); SRI, Sri Lanka; TSM, Tasmania; WAF, Western and Southwestern Africa; WAU, Western Australia. Coastal gradients measured from *Times Atlas of the World* (1985). Passive margin ages from Eldholm & Talwani (1982), Fairbridge (1982), Keen (1982), Lowell *et al.* (1975), Meissner (1986), Salvador (1987), Scrutton (1973), Sweeney (1982), and Veevers (1982).

coastal gradients along sheared passive margins in which continents separate along a transform fault rather than a spreading centre, e.g. eastern Australia (Veevers 1982) and central Norway (Eldholm & Talwani 1982), owing to sharp transitions between continental and oceanic crust and a lack of extensional listric faulting (Scrutton 1982). In contrast, a few coastlines may exhibit anomalously low coastal gradients for their ages. For example, the Libyan coastline of North Africa formed an incompletely sutured embayment during Late Cretaceous collision of the African and European cratons so that its effective age may be greater than that of the youngest (i.e. Palaeocene) rifting event. Unfortunately, such deviations are largely unpredictable for ancient continents, and statistical mean trends (e.g. Fig. 7) must be relied on in the absence of detailed knowledge of palaeo-coastal morphologies.

Hypsometry of ancient continents

Palaeozoic sea level

The effect of area on hypsometric slope is readily demonstrable for present-day landmasses (Fig. 5). This relationship is of particular significance for the determination of Palaeozoic sea levels. Continental areas during the Palaeozoic geotectonic cycle were very different from those of the Mesozoic–Cenozoic cycle (e.g. Ziegler *et al.* 1979). For example, Palaeozoic Gondwana is now fragmented into Africa, Antarctica, Arabia, Australia, South America, and parts of southern Europe and Asia. On the other hand, the tectonic elements of present-day Eurasia formed a number of separate plates during the Palaeozoic, the largest of which were Baltica, China, Kazakhstan, and Siberia. Palaeozoic Laurentia had roughly the same area as present-day North America.

Three Palaeozoic landmasses of markedly different sizes were chosen to evaluate the landmass area effect on sea level estimates (Fig. 8). China, most of which was composed of two independent microplates averaging four million km^2 in area (*Atlas of the Palaeogeography of China* 1985), was a Palaeozoic landmass of microcontinental dimensions. Laurentia, which was about 31 million km^2 in area, was a mid-sized continent, while Gondwana, roughly 105 million km^2 in area, was the largest Palaeozoic landmass. These continents have widely divergent flooding records with China representing maximum (*c.* 30–80%) and Gondwana minimum submergence (*c.* 5–25%; Fig. 8A). To evaluate the sea level record of each of these landmasses correctly requires selection of continental hypsometries on the basis of contemporary, rather than present, landmass area. Hypsometric slope estimates based on the main continental trend (Eq. 5, Appendix) are 4.1 m/%area for China, 5.8 m/%area for Laurentia, and 7.1 m/%area for Gondwana.

These values produce sea level curves for China and Laurentia which are in good general agreement (Fig. 8B). The most salient difference in their sea level histories, the absence of a Cambrian transgressive event in China, probably reflects differing geotectonic histories. The Chinese microplates were not part of a Late Proterozoic proto-Pangea and thus did not participate in the Cambrian rifting event that affected most other continents (Ziegler *et al.* 1979; *Atlas of the Palaeogeography of China* 1985). On the other hand, while the general trends of the Gondwanan sea level record are similar to those for Laurentia (e.g. Middle Cambrian transgression, Siluro–Devonian high-stand, and Permian regression), sea levels calculated for Gondwana are uniformly low throughout the Palaeozoic in relation to the other landmasses (Fig. 8B). Overall, the sea level curves represent a 50–95% reduction in variance with respect to the continental area-flooded curves (Fig. 8C).

The discrepancy in sea level amplitudes between Gondwana and the other continents may be due either to inadequacies in flooding data or to anomalies in coastal hypsometry. Underestimation of Gondwanan flooding during the Palaeozoic is, in fact, likely due to subsequent loss of flooded continental margins. For example, the Tethyan margin of Gondwana was largely transported northward during the Mesozoic as a series of microcontinents which are now incorporated into southern Asia in a belt extending from Turkey to Malaya (Ziegler *et al.* 1979). It is also possible that the Gondwana supercontinent had a fundamentally steeper hypsometry than that predicted by the landmass area effect, perhaps due to crustal thickening or reduction in passive margin length. It is not clear, however, that supercontinents should generally diverge from the main continental trend, and the close conformance of

Fig. 8. Example of sea level determination using hypsometric slope estimates based on the landmass area effect. (**A**) Palaeozoic area-flooded curves for China (*Atlas of the Palaeogeography of China* 1985), Laurentia (Termier & Termier 1952), and Gondwana (Termier & Termier 1952; Wolfart 1967). Gondwana comprises an areally-weighted average of data from Africa, South America, Australia, India, and Southwest Asia. (**B**) Palaeozoic sea level elevations for the same continents. Calculated sea levels based on hypsometric slope estimates of 4.1 m/%area for China, 5.8 m/%area for Laurentia, and 7.1 m/%area for Gondwana. These were calculated from Eq. 2 (Appendix) based on Palaeozoic landmass areas of 4 million km^2 (China), 31 million km^2 (Laurentia), and 105 million km^2 (Gondwana). (**C**) Reduction in variance between area flooded data and calculated sea levels. Variance reduction is calculated as the ratio of variances between data sets normalized to a common mean and averages 55% for the Palaeozoic as a whole.

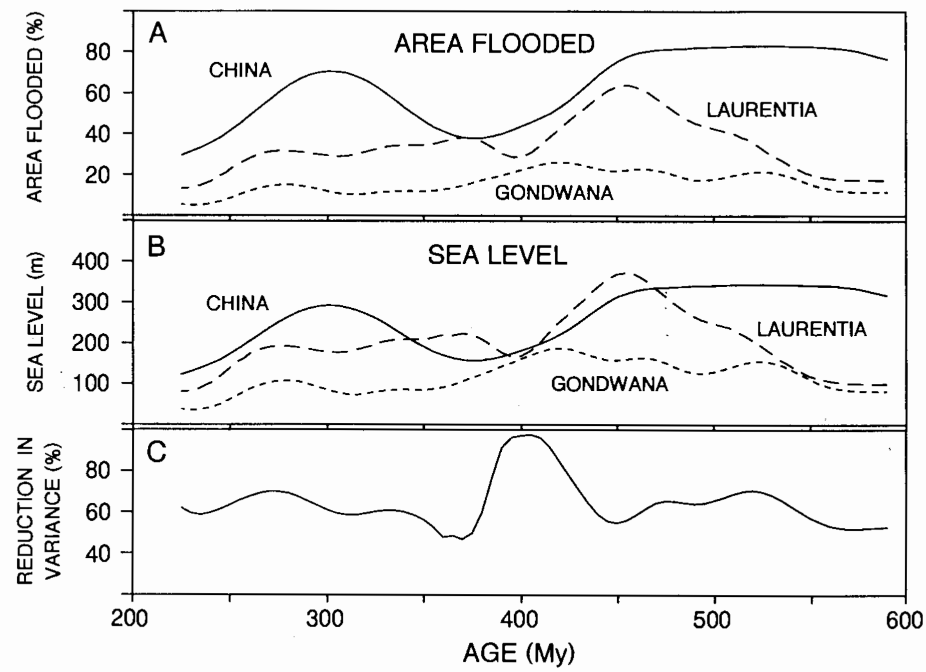

the only extant supercontinent, Eurasia, suggests otherwise (Fig. 5).

An alternative approach to the analysis of Palaeozoic sea levels is possible (Fig. 9). This method assumes (1) that continental flooding primarily records a common eustatic history and (2) that differences in the magnitude of flooding between continents reflect differences in epoch-average hypsometric slopes. The first assumption implies that the eustatic component present in the continental flooding curves can be derived by superimposing area-flooded curves to achieve minimum variance. Residual differences between the curves thus represent the local tectonic or epeirogenic component of the flooding records. The second assumption equates the factors by which the area-flooded curves are adjusted up or down in achieving minimum variance to the ratios between continental hypsometric slopes. Initially, resultant sea level curves are non-dimensional, but they can be scaled by estimating hypsometric slopes for the continents which honour the adjustment ratios previously determined.

Superimposition of Palaeozoic flooding curves result in upward adjustment of the Laurentia curve by a factor of 1.6 and of the Gondwana curve by a factor of 3.2 in relation to the China curve (Fig. 9A). Thus, China, Laurentia, and Gondwana had epoch-average hypsometric slopes with ratios of 1:1.6:3.2, respectively. These ratios can be used to estimate hypsometric slopes for the three landmasses. One method is to choose hypsometric slopes for China (2.7 m/%area), Laurentia (4.2 m/%area), and Gondwana (8.4 m/%area) that minimize cumulative variance around the main continental trend (Fig. 9B, left inset). This assumes that coastal hypsometries of the three continents generally conformed to the main trend but deviated slightly, as do many modern landmasses. An alternative approach is to fit values for China (3.9 m/%area) and Laurentia (6.1 m/%area) to the main trend and assume that Gondwana (12.2 m/%area) had an anomalously steep coastal hypsometry (Fig. 9B, right inset). The resulting sea level scales differ by a factor of 1.4 (Fig. 9B).

Comparison of sea level amplitudes based on estimated palaeo-hypsometries with those of Hallam's (1984) Phanerozoic eustatic curve reveal major differences. Hallam determined a Palaeozoic maximum of +600 m based mainly on flooding data for the Soviet Union (Vinogradov 1967–69, cited in Hallam 1977). As mentioned previously, Palaeozoic Eurasia comprised numerous smaller landmasses (Ziegler *et al.* 1979), and sea level estimates for these continents cannot meaningfully be based on present-day Eurasian or global hypsometry. Our analysis indicates that the magnitude of the Siluro–Ordovician highstand was between +200 m and +400 m, depending on variations in method of calculation, rather than +600 m (Figs 8 & 9). Our estimates for the Deveno–Carboniferous highstand of +100 m to +200 m are also substantially lower than Hallam's +380 m to +400 m.

This example illustrates the utility of hypsometric slopes in eustatic analysis. Much of the variance in flooding between different Palaeozoic continents can be accounted for through correction for changes in landmass area. Further, the resulting sea level estimates are probably superior to previous estimates due to consideration of multiple flooding records. Ideally, flooding records for a large number of palaeo-landmasses could be reconstructed and used to determine hypsometric adjustment ratios. These ratios could then be fitted to the main trend of an area-hypsometric slope plot (e.g. Fig. 5) and continents with anomalous hypsometries identified through their divergence from the pack.

Hypsometry and geotectonic cycles

The dependence of coastal gradient on type and age of continental margin has probably been a major factor

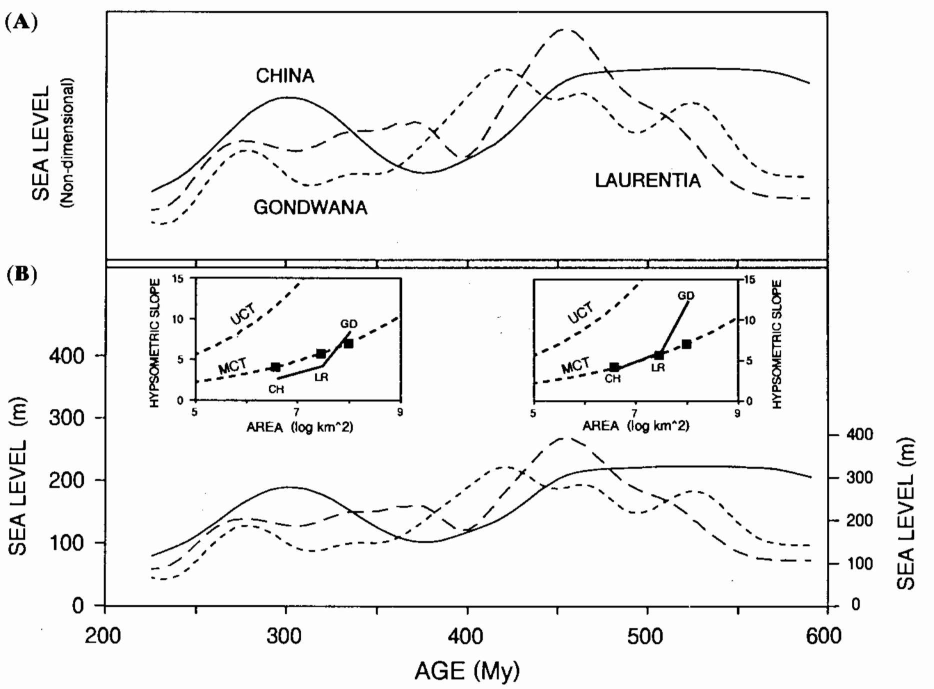

Fig. 9. Example of sea level determination using hypsometric slope ratios based on minimum variance superimposition of area-flooded curves. (**A**) Palaeozoic area-flooded curves for China, Laurentia, and Gondwana adjusted to maximize average variance reduction in resulting sea level curves (80% for Palaeozoic as a whole). These adjustments require hypsometric slopes with ratios of 1:1.6:3.2 for China, Laurentia, and Gondwana, respectively. The ordinate is dimensionless. (**B**) The same curves plotted versus two different sea level scales based on differing estimates of hypsometric slope. The left-hand scale is based on hypsometric slopes with fixed ratios as given above and calculated to have minimum variance around the main continental trend (upper left inset). The right-hand scale is based on hypsometric slopes with fixed ratios for which China and Laurentia conform to the main trend and Gondwana plots in an elevated position (upper right inset). In both insets: CH, China; LR, Laurentia; GD, Gondwana; MCT, main continental trend; UCT, uplifted continental trend; squares indicate hypsometric slope estimates based on landmass area effect as applied in Fig. 8.

contributing to changes in palaeo-hypsometry. Such changes occur as the frequency and age distribution of passive margins for each continent and for the world as a whole evolve through time. As a first approximation, this evolution is cyclic and mirrors plate tectonic phases of continental rifting and collision. During a Pangaean phase, total passive margin length (frequency) is lower than during a rifted phase. A rifting event results in lengthening of passive margins and a shift in the age distribution toward young, steep margins. As continents disperse and passive margins age, the age distribution eventually shifts back toward older, flatter margins, reducing hypsometric slopes and enhancing the 'floodability' of continents. Finally, continental collisons consume passive margins and their total length (frequency) decreases, initiating a new Pangaean phase. Concomitant changes in ocean basin volume through such a geotectonic cycle (not considered here) will reinforce flooding trends associated with continent margin evolution. Ocean basin volume decreases during rift-drift phases due to thinning and lateral extension of continental crust (Wyatt 1986) and to increase in size of mid-ocean ridges (Heller & Angevine 1986), as a consequence of which sea levels are forced higher onto continent margins.

The impact of a geotectonic cycle of this type on continental hypsometry can be evaluated through calculating model hypsometric slopes based on passive margin age-coastal gradient relations. As a first approximation, coastal gradients for any coastline are log-normally distributed (Fig. 6), and mean coastal gradients for passive margins decrease exponentially with age (Fig. 7). Since coastal gradient standard deviations do not show statistically significant age-dependence, the mean standard deviation for the data set (0.42 log m km^{-1}) is used for margins of all ages. These data permit estimation of the most likely distribution of coastal gradients for a passive margin of any given age.

Changes in coastal hypsometry were modelled through a 300 Ma plate tectonic cycle (Fig. 10). The cycle comprises an initial 50 Ma sutured phase with a fixed length of 'active' margin, a 200 Ma rift-drift phase during which an additional increment of passive margin is created, and a 50 Ma collision phase during which the passive margin is consumed. Hypsometric slope is constant during the sutured phase as pre-rift 'active' margins were assigned a coastal gradient distribution representing a combination of active and mature passive margins (Eq. 8, Appendix). Coupling of active and passive margin coastal gradients (e.g. as through thermal uplift) results in an initial increase in hypsometric slope during rifting. Thereafter, hypsometric slope decreases progressively during tthe rift-drift phase due to the age-dependency of passive margin coastal gradients (Fig. 7). Finally, hypsometric slope returns to its pre-rift value as mature passive margins are progressively consumed (e.g. as through oblique convergence along a subduction zone).

Ranges of values for landmass area, passive margin length, shoreline ratio, and active margin coastal gradient representative of modern continents are used to illustrate the possible variation in, and rate of change of, hypsometric slope through a geotectonic cycle (Fig. 10). Correspondence between real and model hypsometric slopes is generally good. North America, South America, and Australia plot well within model limits for continents of their respective areas and passive margin age ranges (Fig. 10B). While Eurasia has a rather low hypsometric slope given its range of passive margin ages, lengthy low-gradient, supermature passive margins along its Arctic coast may skew its hypsometric slope toward unusually low values. Africa, on

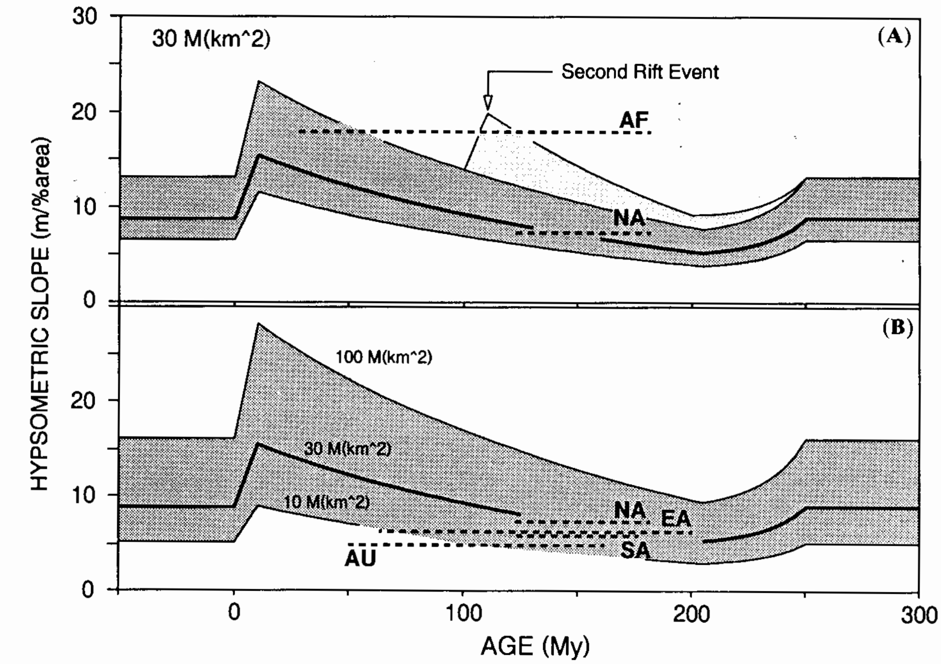

Fig. 10. Evolution of hypsometric slopes through a 300 Ma geotectonic cycle. The model allows variation in landmass area, passive margin length (PSV; given as a percentage of an invariant active margin length), shoreline ratio (SLR), and mean active margin coastal gradient (CG). Hypsometric slopes for modern continents are shown as bars representing age ranges of extant passive margins (abbreviations as in Fig. 5). (**A**) Changes in hypsometric slope for a 30 million km^2 landmass. The heavy middle line employs intermediate values for all parameters: PSV = 30%, SLR = 3.0, CG = 0.5 log m km^{-1}. The upper and lower lines limit the range of possible hypsometric slopes for combinations of model parameters: PSV = 20–40%, SLR = 2.0–4.0, and CG = 0.4–0.6 log m km^{-1}. The effect of a second rift event is shown for a combination of parameters similar to those for Africa. Modern landmass areas: North America = 25.3 million km^2, Africa = 30.3 million km^2. (**B**) Changes in hypsometric slope for landmasses of 10, 30, and 100 million km^2 employing intermediate values for model parameters. Modern landmass areas: Australia = 8.9 million km^2, South America = 17.6 million km^2, Eurasia = 54.1 million km^2. The heavy lines in (**A**) and (**B**) represent the same combination of model parameters.

the other hand, has an exceptionally high hypsometric slope, an anomaly which may be atttibutable to its geotectonic history of multiple rift events (Fig. 10A). Evidence that Africa is currently undergoing rift-related thermal uplift supports this interpretation (Bond 1978*b*).

Such a model permits several general observations of significance. First, through the course of a geotectonic cycle, hypsometric slope changes by a factor of two to three under most combinations of model parameters. As a consequence, continental 'floodability', i.e. the rate at which a landmass is potentially flooded or exposed, is two to three times greater at the end of a rift–drift phase than at its beginning. Second, at any point within the geotectonic cycle, the range of possible hypsometric slopes for a landmass of given area is relatively large (Fig. 10A). Therefore, it is not possible to estimate hypsometric slope from position within a geotectonic cycle alone. Knowledge of hypsometric slope at some point within the cycle (e.g. the present) may permit projection of changes in hypsometric slope (e.g. into the past or future), especially if data regarding continent margin events are available. Such projection must remain tentative as vertical continental motions due to local tectonic, thermal, or isostatic disturbances can alter coastal hypsometries in an unpredictable manner on geologically short timescales.

Conclusions

The most important determinants of coastal hypsometry are landmass area and coastal gradient. Increases in either parameter result in steeper area-elevation distributions. As a consequence, any given change in sea level will flood or expose a smaller fractional area of continents which are large or have steep coastal gradients than of those which are small or have gentle coastal gradients. Coastal gradients are dictated primarily by the tectonic setting and age of continental margins. While active and transform margins generally have steep coasts, mean coastal gradients for passive margins decrease exponentially with increasing margin age. Consequently, continents comprised mostly of mature passive margins are generally more 'floodable'.

These observations are applicable to several problematic aspects of palaeo-eustasy. Hypsometries corrected for changes in landmass area reduce variance in flooding records between different Palaeozoic continents by more than 50%. Recalculated Palaeozoic sea level maxima are between +200 m and +400 m with respect to present sea level, substantially reducing previous estimates of +600 m. Modelling of changes in continental hypsometry due to increasing passive margin age suggests that coastal hypsometries change by a factor of two to three through geotectonic cycles. Thus, sea level highstands associated with times of continent dispersal may result in part from the enhanced 'floodability' of rifted continents.

The authors would like to extend special thanks to L. Albertzart for her dedicated assistance in compilation of palaeogeographic data used here. They also thank S. Boss and P. Howell of the University of Michigan, A. Hallam of the University of Birmingham, and A.

G. Smith of Cambridge University for critically reviewing the manuscript and offering insightful comments and suggestions. Research on patterns of Phanerozoic sediment accumulation at the University of Michigan is supported by the National Science Foundation, NSF grants EAR-86-07970 and EAR-88-03910.

Appendix: Mathematical relationships of model hypsometric controls

A model landmass of conical form permits mathematical definition of hypsometric slope. Whether or not the side of the cone steepens above its base (as do real landmasses) is irrelevant, as we are interested only in the basal section. By definition, hypsometric slope is the rate of change in elevation with respect to fractional land area. For operational reasons, it is calculated over some elevation range of interest:

$$HS = X/[(AR_x/AR_t) \times 100] \tag{1}$$

where HS = hypsometric slope (m/%area)
X = elevation range (m)
AR_x = area within elevation range X (km^2)
AR_t = total area (km^2)

The area within some elevation range of interest is a function of elevation range size, shore length, and coastal gradient:

$$AR_x = X \times SL/CG \tag{2}$$

where SL = shore length (km)
CG = coastal gradient (m/km)
This assumes that the shore-parallel width of elevation range X does not decrease inland, i.e. that radius of shoreline curvature is large in relation to coastal zone breadth, an assumption which is valid for first-order shorelines of continent-sized landmasses. Substituting for AR_x yields:

$$HS = (AR_t \times CG)/(SL \times 100) \tag{3}$$

Shore length is dependent on total area as it cannot be less than the circumference of a circle of equivalent area. An independent parameter termed 'shoreline ratio', or the ratio of shore length to the circumference of a circle of equivalent area, can be defined. It ranges in value from 1.0 for a circular landmass to converging on infinity for landmasses of increasingly irregular shape. Its relationship to shore length is:

$$SL = SLR \times 2 \times \sqrt{(\pi \times AR_t)} \tag{4}$$

where SLR = shoreline ratio (non-dimensional)

Substituting shoreline ratio for shore length and rearranging yields an equation in which hypsometric slope is a function of independent size, shape, and steepness parameters (e.g. Fig. 4):

$$HS = \frac{CG \times \sqrt{AR_t}}{200 \times SLR \times \sqrt{\pi}}$$

The empirically-fit trend lines of Fig. 5 are calculated with a modified form of Eq. (5) in which coastal gradient is not invariate but changes as a function of landmass area:

$$HS = \frac{CG \times \sqrt{AR_t} \times (k \times AR_t)^n}{200 \times SLR \times \sqrt{\pi}} \tag{6}$$

where n determines the rate of change of coastal gradient with respect to landmass area and k is an arbitrary scaling constant. For the uplifted and main continental trends, $n = -0.33$ and, thus, coastal gradient increases inversely with the cube root of landmass area.

Where a landmass has two or more margin types with different coastal gradients, the area within the elevation range of interest is determined separately for each margin type and summed in order to arrive at hypsometric slope:

$$HS = X/\{[(AR_{x1} + AR_{x2}) \times AR_t]/100\} \tag{7}$$

or

$$HS = AR_t/[(SL_1/CG_1 + SL_2/CG_2) \times 100] \tag{8}$$

This permits calculation of hypsometric slopes for model landmasses for which active and passive margin coastal gradients differ and passive margin shore length changes through time (e.g. Fig. 10).

References

Atlas of the Palaeogeography of China. 1985. Cartographic Publishing House, Beijing.

Berner, R. A., Lasaga, A. C. & Garrels, R. M. 1983. The carbonate-silicate geochemical cycle and its effect on atmospheric carbon dioxide over the past 100 million years. *American Journal of Science*, **283**, 641–683.

Bloom, A. L. 1978. *Geomorphology*. Prentice-Hall, Englewood Cliffs, New Jersey.

Bond, G. 1978*a*. Speculations on real sea-level changes and vertical motions of continents at selected times in the Cretaceous and Tertiary Periods. *Geology*, **6**, 247–250.

—— 1978b. Evidence for Late Tertiary uplift of Africa relative to North America, South America, Australia and Europe. *Journal of Geology*, **86**, 47–65.

Carmichael, I. S. E., Turner, F. J. & Verhoogen, J. 1974. *Igneous Petrology*. McGraw-Hill, New York.

Cogley, J. G. 1985. Hypsometry of the continents. *Zeitschrift für Geomorphologie, Supplement band*, **53**.

Eldholm, O. & Talwani, M. 1982. The passive margins of northern Europe and East-Greenland. *In*: Scrutton, R. A. (ed.) *Dynamics of Passive Margins*. Geodynamics Series. American Geophysical Union, Washington DC, **6**, 30–44.

Fairbridge, R. W. 1982. The fracturing of Gondwanaland. *In*: Scrutton, R. A. & Talwani, M. (eds) *The Ocean Floor*. J. Wiley & Sons, Chichester 229–235.

Forney, G. G. 1975. Permo-Triassic sea-level change. *Journal of Geology*, **83**, 773–779.

Hallam, A. 1977. Secular changes in marine inundation of USSR and North America through the Phanerozoic. *Nature*, **269**, 769–772.

—— 1984. Pre-Quaternary sea-level changes. *Annual Review of Earth and Planetary Science*, **12**, 205–243.

Hao, B. U., Hardenbol, J. & Vail, P. R. 1987. Chronology of fluctuating sea levels since the Triassic. *Science*, **235**, 1156–1167.

Harrison, C. G. A., Brass, G. W., Saltzman, E., Sloan, J., II, Southam, J. & Whitman, J. M. 1981. Sea level variations global sedimentation rates and the hypsographic curve. *Earth and Planetary Science Letters*, **54**, 1–16.

——, Miskell, K. J., Brass, G. W., Saltzman, E. S. & Sloan, J. L., II. 1983. Continental hypsography. *Tectonics*, **2**, 357–377.

Heller, P. L. & Angevine, C. L. 1985. Sea-level cycles during the growth of Atlantic-type oceans. *Earth and Planetary Science Letters*, **75**, 417–426.

Inman, D. L. & Nordstrom, C. E. 1971. On the tectonic and morphologic classification of coasts. *Journal of Geology*, **79**, 1–21.

Keen, C. E. 1982. The continental margins of eastern Canada: A review. *In*: Scrutton, R. A. (ed.) *Dynamics of Passive Margins*. Geodynamics Series. American Geophysical Union, Washington DC, **6**, 45–58.

Kinsman, D. J. J. 1975. Rift valley basins and sedimentary history of trailing continental margins. *In*: Fischer, A. G. & Judson, S. (eds) *Petroleum and Global Tectonics*. Princeton University Press, 83–126.

Kossinna, E. 1933. Die Erdoberfläche. *In*: Gutenberg, B. (ed.) *Handbuch der Geophysik, Aufbau der Erde*. Gebrüder Borntraeger, Berlin, **2**, 869–954.

Lowell, J. D., Genik, G. J., Nelson, T. H. & Tucker, P. M. 1975. Petroleum and plate tectonics of the southern Red Sea. *In*: Fischer, A. G. & Judson, S. (eds) *Petroleum and Global Tectonics*. Princeton University Press, 129–153.

Meissner, R. 1986. *The Continental Crust: A Geophysical Approach*. International Geophysical Series. Academic Press, Orlando, Florida, **34**.

Ollier, C. D. & Marker, M. E. 1985. The Great Escarpment of southern Africa. *Zeitschrift für Geomorphologie, Supplementband*, **54**, 37–56.

Pain, C. F. 1985. Morphotectonics of the continental margins of Australia. *Zeitschrift für Geomorphologie, Supplementband*, **54**, 23–35.

Pitman, W. C., III. 1978. Relationship between eustacy and stratigraphic sequences of passive margins. *Geological Society of America Bulletin*, **89**, 1389–1403.

Salvador, A. 1987. Late Triassic–Jurassic paleogeography and origin of

Gulf of Mexico basin. *Bulletin of the American Association of Petroleum Geologists,* **71,** 419–451.

SCHOPF, T. J. M. 1974. Permo–Triassic extinctions: Relation to sea-floor spreading. *Journal of Geology,* **82,** 129–143.

SCRUTTON, R. A. 1973. The age relationship of igneous activity and continental break-up. *Geological Magazine,* **110,** 227–234.

—— 1982. Crustal structure and development of sheared passive continental margins. *In*: SCRUTTON, R. A. (ed.) *Dynamics of Passive Margins.* Geodynamics Series. American Geophysical Union, Washington DC, **6,** 133–40.

SHANMUGAM, G. & MOIOLA, R. J. 1982. Eustatic control of turbidites and winnowed turbidites. *Geology,* **10,** 231–35.

SWEENEY, J. F. 1982. Structure and development of the polar margin of North America. *In*: SCRUTTON, R. A. (ed.) *Dynamics of Passive Margins,* Geodynamics Series. American Geophysical Union, Washington DC, **6,** 17–29.

TERMIER, H. & TERMIER, G. 1952. *Histoire Geologique de la Biosphere.* Masson, Paris.

The Times Atlas of the World, 7th ed. 1985. New York, Times Books.

VAIL, P. R., MITCHUM, R. M., Jr. & THOMPSON, S., III. 1977. Global cycles of relative changes of sea level. *In*: PAYTON, C. E. (ed.) *Seismic Stratigraphy and Global Changes of Sea Level.* Memoirs of the American Association of Petroleum Geologists, **26,** 83–97.

VEEVERS, J. J. 1982. Australian rifted margins. *In*: SCRUTTON, R. A. (ed.) *Dynamics of Passive Margins.* Geodynamics Series. American Geophysical Union, Washington DC, **6,** 72–89.

WISE, D. U. 1974. Continental margins, freeboard and the volumes of continents and oceans through time. *In*: BURK, C. A. & DRAKE, C. L. (eds) *The Geology of Continental Margins.* Springer-Verlag, New York, 45–58.

WOLFART, R. 1967. Zur Entwicklung der paelaozoischen Tethys in vorderasien. *In*: SONNENFELD, P. (ed.) *Tethys: The Ancestral Mediterranean* Benchmark Papers in Geology. Hutchinson Ross, Stroudsburg, Pennsylvania, **53,** 58–70.

WORSLEY, T. R., NANCE, D. & MOODY, J. B. 1984. Global tectonics and eustasy for the past 2 billion years. *Marine Geology,* **58,** 373–400.

WYATT, A. R. 1986. Post-Triassic continental hypsometry and sea level. *Journal of the Geological Society, London,* **143,** 907–910.

—— 1987. Shallow water areas in space and time. *Journal of the Geological Society, London,* **144,** 115–120.

ZIEGLER, A., SCOTESE, C., MCKERROW, W., JOHNSON, M. & BAMBACH, R. 1979. Paleozoic paleogeography. *Annual Reviews of Earth and Planetary Science,* **7,** 473–502.

Received 19 November 1990; revised typescript accepted 10 December 1990.